

## Electronic transport and thermal and optical properties of $\text{Ca}_{1-x}\text{La}_x\text{B}_6$

P. Vonlanthen, E. Felder, L. Degiorgi, and H. R. Ott

*Laboratorium für Festkörperphysik, Eidgenössische Technische Hochschule Zürich, CH-8093 Zürich, Switzerland*

D. P. Young, A. D. Bianchi, and Z. Fisk

*National High Magnetic Field Laboratory, Florida State University, 1800 East Paul Dirac Drive, Tallahassee, Florida 32306*

(Received 24 February 2000; revised manuscript received 5 July 2000)

We present a study of transport, thermal, and optical properties of stoichiometric  $\text{CaB}_6$  and La-doped  $\text{CaB}_6$ . For stoichiometric  $\text{CaB}_6$  a strong increase of the resistivity with decreasing temperature and anomalies in the low-temperature behavior of the resistivity and the specific heat have been observed. The application of an external magnetic field at low temperatures is shown to lead to an anomalous magnetoresistance in the case of stoichiometric  $\text{CaB}_6$ . The optical conductivity exhibits a strong doping dependence. Rather unexpectedly, small changes in the chemical composition lead to significant changes in the electronic interband transitions in the visible-UV spectral range. The relevance of our results with respect to the recently suggested excitonic scenario for explaining the physical properties of alkaline-earth hexaborides is discussed.

### I. INTRODUCTION

Recent thermal and transport measurements on alkaline-earth hexaborides have revealed unexpected features in their physical properties.<sup>1-3</sup> The most remarkable observation has been that  $\text{Ca}_{1-x}\text{La}_x\text{B}_6$  with  $x \approx 0.01$ , i.e., lightly doped with electrons, shows an itinerant type of ferromagnetic order, stable up to temperatures of the order of 600–900 K.<sup>1,3</sup> Previously,  $\text{SrB}_6$  has been shown<sup>2</sup> to be at the border separating semimetals from insulators. This finding was confirmed by band structure calculations revealing a very peculiar configuration of the electronic excitation spectrum,<sup>4</sup> with a faint overlap of the valence and conduction bands in a tiny region in  $k$  space around the  $X$  points of the Brillouin zone. The discovery of weak ferromagnetism in the electron-doped alkaline-earth hexaborides has renewed the theoretical interest in magnetism at low electron densities,<sup>5</sup> and particularly in the so-called excitonic transition,<sup>6-9</sup> where a semimetal with a small overlap or a semiconductor with a small band gap can develop into an excitonic insulator involving a Bose condensate of excitons.<sup>9</sup> Weak ferromagnetism is then due to a spontaneous time reversal symmetry breaking upon doping.

The present work mainly aims at presenting additional information on the stoichiometric binary compound  $\text{CaB}_6$  in the absence of doping, and at discussing the physical properties of  $\text{CaB}_6$  in relation to an excitonic instability. As vacancies are very likely to be present in hexaborides,<sup>10</sup> special precautions were taken to prepare material close to being perfectly stoichiometric. Furthermore, doped  $\text{CaB}_6$  samples (by La doping or via metal vacancies) have been studied to obtain information on the effect of doping on an excitonic insulator.

### II. SAMPLES AND EXPERIMENTAL METHODS

Different single-crystalline  $\text{CaB}_6$  samples have been investigated. All of them were prepared by solution growth from Al flux, using the necessary high-purity elements as

starting materials. Hexaborides have the tendency to end up as boron rich by the formation of metal vacancies, but they are essentially stoichiometric at the metal-rich phase boundary.<sup>10</sup> The sample of  $\text{CaB}_6$  that was investigated in great detail in this study was prepared by starting the flux-growth synthesis with a mixture containing an extra amount  $\delta$  of Ca. In the following this particular sample, which is close to being stoichiometric, is denoted as  $\text{Ca}_{1+\delta}\text{B}_6$ . The other samples that have been investigated include one  $\text{CaB}_6$  sample where the flux-growth synthesis was started without an extra amount of Ca and therefore some metal vacancies are likely to be present. These defects are the most likely cause of the enhanced conductivity of metal-deficient material. Furthermore, we studied two samples where 0.5% and 1%, respectively, of the divalent Ca atoms had been replaced by trivalent La.

The electrical resistivity was measured between 35 mK and 300 K, using a four-probe low-frequency ac technique. The measurements in magnetic fields were made using a transverse configuration, i.e., with the external magnetic field  $\vec{H}$  applied perpendicularly to the direction of the electrical current  $\vec{I}$ . The specific heat was measured between 80 mK and 20 K, using a relaxation-type method. All our samples for the resistivity measurements were platelets with rectangular shapes and typical dimensions of 0.5 mm  $\times$  1 mm  $\times$  5 mm. The samples for the specific heat and optical measurements, always picked from the same batch as the sample used for the resistivity measurements, had typical weights of the order of a few milligrams. Measurements of the magnetization were performed using a commercial superconducting quantum interference device (SQUID) magnetometer. For all the measurements, conventional <sup>4</sup>He cryostats were used in the temperature range above 1.4 K and a dilution cryostat for reaching temperatures below 1.4 K.

The optical reflectivity was measured in a broad frequency range, extending from the far infrared up to the ultraviolet, i.e., from 15 to 10<sup>5</sup> cm<sup>-1</sup>, and at various temperatures. The experimental setup has been described in detail in

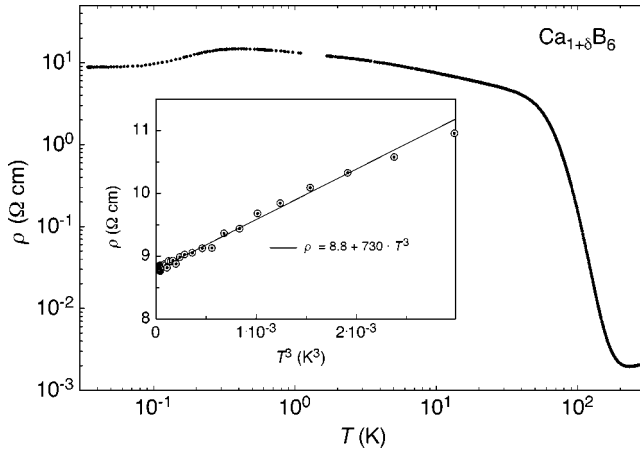


FIG. 1.  $\rho(T)$ , the resistivity of  $\text{Ca}_{1+\delta}\text{B}_6$  as a function of the temperature on double logarithmic scales. Inset:  $\rho(T^3)$ , emphasizing the  $T^3$  dependence of the electrical resistivity at very low temperatures.

Ref. 2. The optical conductivity is obtained via a Kramers-Kronig transformation of the reflectivity spectra, employing the usual extrapolation schemes at low and high frequencies.<sup>11</sup>

### III. EXPERIMENTAL RESULTS

Most of the experimental results presented in this paper were obtained for the  $\text{Ca}_{1+\delta}\text{B}_6$  sample. To our knowledge this is the first study clearly demonstrating the quasisemiconducting behavior of close to stoichiometric  $\text{CaB}_6$  material in a wide temperature range below 230 K. Furthermore, experimental results on electron-doped  $\text{CaB}_6$  are presented.

#### A. Electrical transport

In Fig. 1 the resistivity  $\rho(T)$  of  $\text{Ca}_{1+\delta}\text{B}_6$  is plotted as a function of the temperature  $T$  on double logarithmic scales. The resistivity shows very pronounced  $T$  dependences in different  $T$  regimes. Below room temperature the resistivity first drops continuously, indicating a low but metallic conductivity. It reaches a minimum of  $0.002 \text{ } \Omega \text{ cm}$  around 230 K, a reduction of about 8% in comparison with the resistivity at room temperature. Below 230 K,  $\rho(T)$  increases by about four orders of magnitude and reaches a maximum of  $14.8 \text{ } \Omega \text{ cm}$  at 0.4 K, below which a reduction of about 40% of the resistivity is observed. The temperature derivative of  $\rho(T)$ , not presented explicitly, is positive above 230 K, negative between 230 K and 0.4 K, turning positive again below 0.4 K and finally tending to zero below 50 mK, thus indicating a nonzero constant conductivity close to  $T = 0 \text{ K}$ . The very high ratio of low-temperature to room-temperature resistivity of about  $1 \times 10^4$  may be interpreted as an indication of a very low density of Ca sublattice vacancies. The inset of Fig. 1 shows that  $\rho(T)$  varies as  $T^3$  for  $T \rightarrow 0 \text{ K}$  and the resistivity reaches a residual resistivity of  $\rho_0 = 8.8 \text{ } \Omega \text{ cm}$ . The magnitude of the prefactor of the  $T^3$  term is, at  $730 \text{ } \Omega \text{ cm/K}^3$ , enormous.

The influence of an external magnetic field on the resistivity of  $\text{Ca}_{1+\delta}\text{B}_6$  below 1.2 K is illustrated in Fig. 2. The data resulted from temperature scans at several magnetic

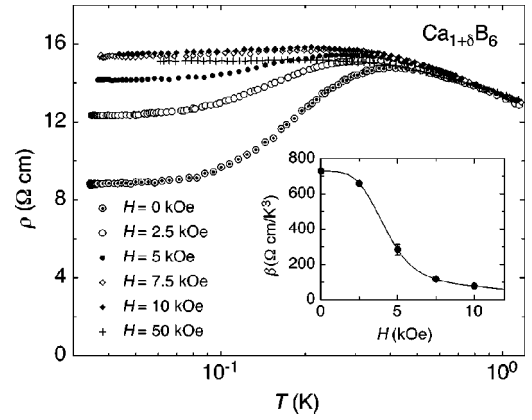


FIG. 2.  $\rho(T, H)$ , the resistivity of  $\text{Ca}_{1+\delta}\text{B}_6$  as a function of the temperature in a semilogarithmic plot for different applied magnetic fields between 0 and 50 kOe. Inset: Field dependence of the parameter  $\beta$  of the equation  $\rho(T) = \rho_0 + \beta T^3$  (see text).

fields  $H$ , i.e.,  $H = 0, 2.5 \text{ kOe}, 5 \text{ kOe}, 7.5 \text{ kOe}, 10 \text{ kOe}$ , and  $50 \text{ kOe}$ . It can be seen that the application of moderate external magnetic fields tends to suppress the decrease of the resistivity below 0.4 K. Below 0.15 K the resistivity can best be approximated by the sum of two terms  $\rho(T) = \rho_0 + \beta T^3$ , where both  $\rho_0$  and  $\beta$  vary with the magnetic field. In the inset of Fig. 2 the coefficient  $\beta$  is plotted versus  $H$ . The solid line is a guide to the eye. The prefactor of the  $T^3$  term already decreases by an order of magnitude for moderately intense magnetic fields. Although not shown explicitly here, we note that the temperature of the maximum in the resistivity,  $T_{\text{max}}$ , for different applied magnetic fields between 0 and 10 kOe decreases as  $T_{\text{max}}(\text{K}) = 0.394 - 0.018H$  ( $H$  in kOe), i.e., linearly, as a function of the applied magnetic field.

In Fig. 3 the normalized magnetoresistance  $[\rho(H) - \rho(0)]/\rho(0)$  of  $\text{Ca}_{1+\delta}\text{B}_6$  is plotted for three different temperatures 0.1, 0.25, and 0.4 K. The most pronounced variation of  $\rho(H)$  is observed at the lowest of these temperatures. For all three temperatures the magnetoresistance is positive and shows a maximum around 13 kOe. This magnetic field corresponds approximately to the value where the coefficient  $\beta$  in  $\rho(T)$  vanishes. At 100 mK the maximum of the normalized magnetoresistance reaches 65%.

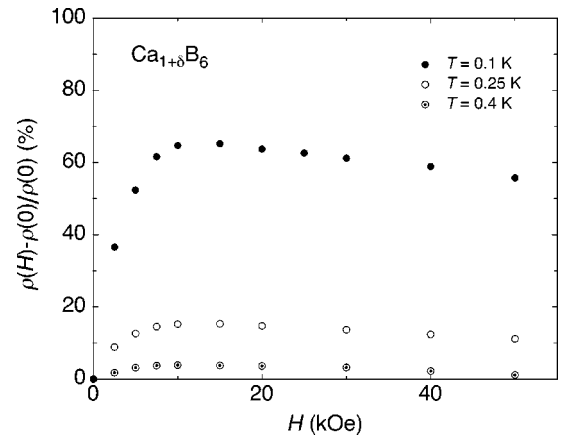


FIG. 3. Magnetoresistance in a transverse configuration of  $\text{Ca}_{1+\delta}\text{B}_6$  for three different temperatures below 1 K.

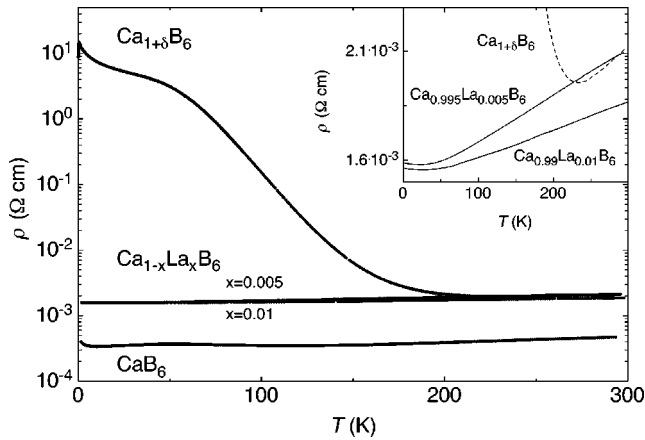


FIG. 4.  $\rho(T)$ , the resistivity as a function of the temperature for  $\text{Ca}_{1+\delta}\text{B}_6$ ,  $\text{CaB}_6$  (taken from Ref. 12) and  $\text{Ca}_{1-x}\text{La}_x\text{B}_6$  ( $x=0.005$  and  $0.01$ ). Inset: Part of the data plotted on a linear scale.

The resistivity curve of the  $\text{CaB}_6$  sample where the flux-growth synthesis was started without an extra amount of Ca has previously been described by Paschen *et al.*<sup>12</sup> It shows an overall lower resistivity than the  $\text{Ca}_{1+\delta}\text{B}_6$  sample, and has a rather complicated shape, i.e., the resistivity decreases below room temperature, passes through two minima and a maximum, and finally increases again toward the lowest temperatures.

The doping of  $\text{CaB}_6$  with La has been shown<sup>1,3</sup> to have drastic consequences. In the inset of Fig. 4 the resistivities  $\rho(T)$  of  $\text{Ca}_{1-x}\text{La}_x\text{B}_6$  with  $x=0.5\%$  and  $x=1\%$  are plotted. Both samples show a metallic behavior below 300 K. In the case of  $x=0.5\%$ , the room-temperature resistivity is  $\rho = 2.1 \times 10^{-3} \Omega \text{ cm}$  and  $\rho(T)$  decreases linearly as a function of temperature down to 80 K, where it starts to flatten off, reaching a minimum value of  $\rho = 1.6 \times 10^{-3} \Omega \text{ cm}$  around 25 K; finally, toward the lowest temperatures, it increases slightly again by about 0.5%. The application of an external magnetic field of about 30 kOe in a transverse configuration results in a suppression of the slight increase of the resistivity below 25 K, i.e., the resistivity around 1.5 K in an applied magnetic field exceeding 30 kOe is the same as in zero field at 25 K. The second sample with  $x=1\%$  shows a very similar behavior, with slightly smaller absolute values of the resistivity. In Fig. 4 the resistivity curves of the different  $\text{CaB}_6$  samples have been plotted for comparison. It can be seen that a small amount of La doping induces a drastic change in the resistivity below room temperature. The overall resistivity of the La doped samples is larger than for the Ca deficient crystal, most likely indicating that some disorder is induced by La doping.

### B. Specific heat

In Fig. 5 we present our specific heat data for  $\text{Ca}_{1+\delta}\text{B}_6$  as a function of temperature between 80 mK and 20 K. Below 20 K, the specific heat  $C_p(T)$  decreases with decreasing temperature as commonly expected. Below 1 K, however, the specific heat increases with decreasing temperature and, after reaching a maximum at 0.3 K, finally decreases again below that temperature. The lattice contribution to the specific heat may, as usual, be evaluated by plotting  $C_p/T$  versus  $T^2$  as

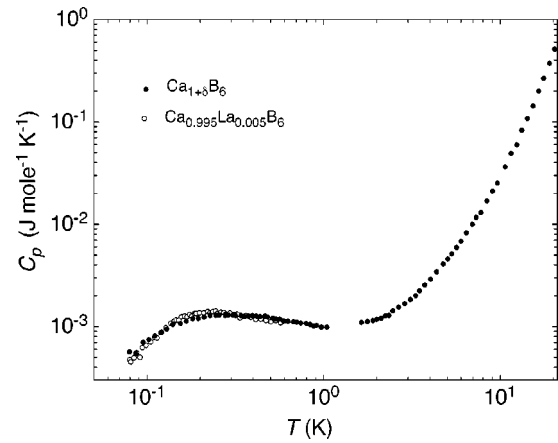


FIG. 5. Low-temperature specific heat of  $\text{Ca}_{1+\delta}\text{B}_6$  and  $\text{Ca}_{0.995}\text{La}_{0.005}\text{B}_6$  as a function of temperature between 80 mK and 20 K.

shown in Fig. 6. The solid line, extrapolating to zero at  $T=0$  and representing the low-temperature phonon specific heat below 11 K, is compatible with a vanishing electronic contribution to  $C_p(T)$  at temperatures above 8 K. The plot reveals, however, a significant excess specific heat below 7 K. From the slope of the solid line in Fig. 6, a measure of the lattice contribution to the specific heat,  $C_{\text{ph}}$ , we may calculate the Debye temperature  $\Theta_D$ , and we obtain  $\Theta_D = 783$  K. The same plot reveals an excess specific heat below about 7 K. The inset of Fig. 6 shows the low-temperature part of  $C_p/T$  below 0.5 K. It can be seen that  $C_p/T$  increases monotonically down to 0.15 K where it saturates at a value of approximately  $7 \text{ mJ mol}^{-1} \text{ K}^{-2}$ . The cause of this excess specific heat is not clear at present, but has previously been observed in a similar manner for  $\text{SrB}_6$ ,<sup>2</sup> and is obviously also present in La-doped  $\text{Ca}_{0.995}\text{La}_{0.005}\text{B}_6$  (see Fig. 5).

From the excess specific heat, the excess entropy below 8 K may be calculated. It saturates around 8 K at a value of  $4.7 \text{ mJ mol}^{-1} \text{ K}^{-1}$ , i.e., less than 0.1% of  $R \ln 2$ .

### C. Magnetization

In Fig. 7 the magnetization versus applied magnetic field is plotted for  $\text{Ca}_{1+\delta}\text{B}_6$  and for a  $\text{CaB}_6$  sample with metal

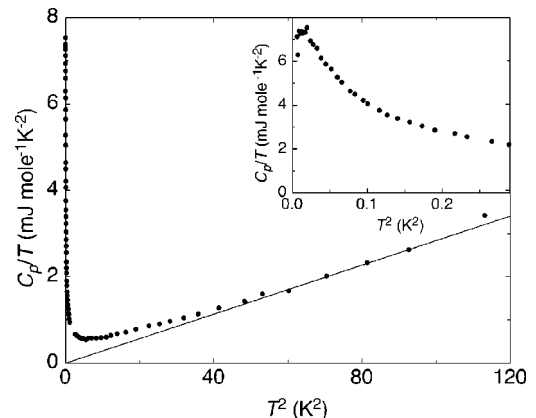


FIG. 6.  $C_p/T$  vs  $T^2$  for  $\text{Ca}_{1+\delta}\text{B}_6$  below 11 K. The solid line represents the estimated lattice contribution to the specific heat,  $C_{\text{ph}}$ .

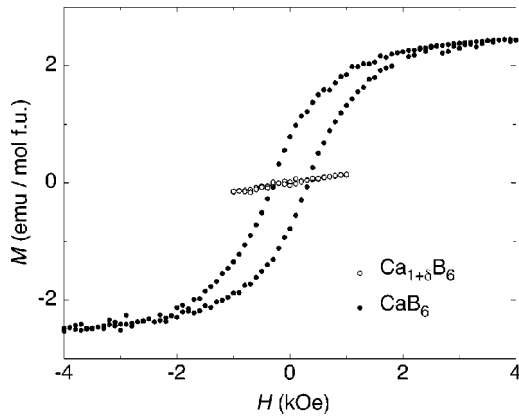


FIG. 7. Magnetization per mole of compound versus applied field for  $\text{CaB}_6$  and  $\text{Ca}_{1+\delta}\text{B}_6$ . The data for  $\text{CaB}_6$  were taken at 30 K and for  $\text{Ca}_{1+\delta}\text{B}_6$  at 2 K.

vacancies. The presence of metal vacancies in the  $\text{CaB}_6$  sample may be deduced from the electrical resistivity of this particular sample, not shown here, which below 80 K is more than two orders of magnitude smaller than for the  $\text{Ca}_{1+\delta}\text{B}_6$  sample. The data shown for the  $\text{CaB}_6$  sample were taken at 30 K and those for the  $\text{Ca}_{1+\delta}\text{B}_6$  sample at 2 K. The sample with metal vacancies is ferromagnetic, as can clearly be inferred from the hysteresis loop in the magnetization curve. It has been verified that this hysteresis loop is essentially temperature independent between 2 and 300 K. On the other hand, in the case of the  $\text{Ca}_{1+\delta}\text{B}_6$  sample, no trace of ferromagnetism at any temperature between room temperature and 2 K could be observed. The tiny signal observed at the lower end of the covered temperature regime is of the order of the background signal. Naturally, the observation that close to stoichiometric  $\text{CaB}_6$  does not reveal any ferromagnetic order down to low temperatures is one of the key results of this work.

#### D. Optical properties

Figure 8 shows the reflectivity spectra of  $\text{Ca}_{1+\delta}\text{B}_6$  and  $\text{Ca}_{1-x}\text{La}_x\text{B}_6$  ( $x=0.5\%$  and  $1\%$ ) and the corresponding real part of the optical conductivity at 300 K. We have not found any significant temperature dependence in the optical spectra of these compounds between 300 and 6 K. A remarkable feature in the optical reflectivity of  $\text{Ca}_{1-x}\text{La}_x\text{B}_6$  is the absence of the plasma edge, seen at about  $3000\text{ cm}^{-1}$  in the  $\text{SrB}_6$  compound (see Fig. 6 in Ref. 2). Several absorptions appear in  $R(\omega)$  of  $\text{Ca}_{1-x}\text{La}_x\text{B}_6$ , notably a broad and very intense peak at  $150\text{ cm}^{-1}$  and a weak but sharp signal around  $860\text{ cm}^{-1}$ , indicated by an arrow in Fig. 8(a). Both features are most likely related to phonon modes. The mode around  $150\text{ cm}^{-1}$  appears at a lower energy than the  $200\text{ cm}^{-1}$  expected from the mass renormalization of the corresponding frequency in  $\text{CsI}$ ,<sup>13</sup> assuming doubly charged ions. This type of estimate is quite successful for identifying this phonon mode of  $\text{SrB}_6$  (Ref. 2) and  $\text{EuB}_6$ .<sup>14</sup> The mode at  $860\text{ cm}^{-1}$  reflects the intramolecular-type vibration of the B octahedra, typical for the hexaboride lattice.<sup>14</sup> Besides these phonon modes, two additional absorptions appear in  $R(\omega)$ . For  $\text{Ca}_{1+\delta}\text{B}_6$ , there are two narrow features adjacent to the high-frequency tail of the optical phonon at  $150\text{ cm}^{-1}$  [see

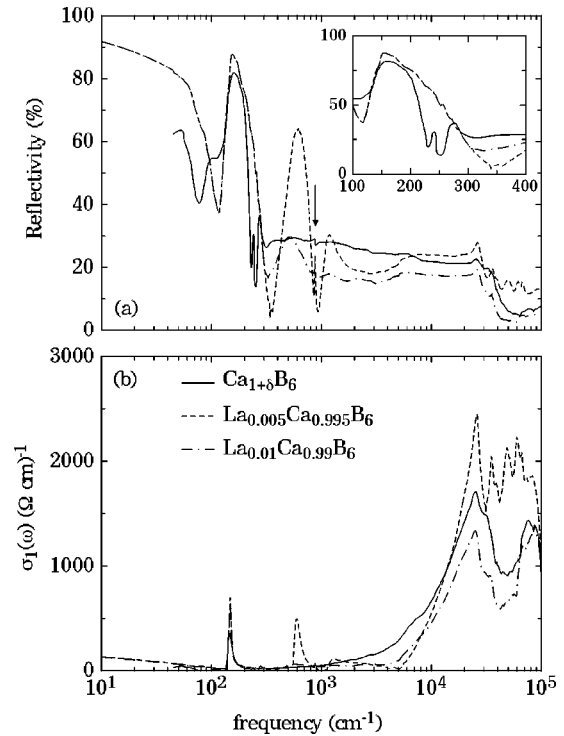


FIG. 8. (a) Reflectivity spectra and (b) the corresponding real parts of the optical conductivity  $\sigma_1(\omega)$  of  $\text{Ca}_{1+\delta}\text{B}_6$ ,  $\text{Ca}_{0.995}\text{La}_{0.005}\text{B}_6$ , and  $\text{Ca}_{0.99}\text{La}_{0.01}\text{B}_6$  at 300 K. Note the logarithmic frequency scale. Inset: low-frequency part of the reflectivity spectra. The arrow in (a) indicates a phonon mode (see text).

inset of Fig. 8(a)]. Whereas for the 0.5% La-doped compound we clearly recognize two strong absorptions at about  $700\text{ cm}^{-1}$  and  $1200\text{ cm}^{-1}$ , these are quite damped and broad for the 1% La-doped compound.

At this point we note that the results of reflectivity measurements in the far infrared (FIR) on a Ca-deficient  $\text{CaB}_6$  sample are very similar to those obtained for  $\text{Ca}_{1+\delta}\text{B}_6$ , although the temperature dependences of the respective resistivities  $\rho(T)$  are substantially different (see Fig. 4). Quite generally,  $R(\omega)$  is lower for the Ca-deficient crystal in the visible and UV spectral ranges, where the electronic interband transitions develop (see below). Our spectra for both  $\text{CaB}_6$  crystals are distinctly different from previously published results, obtained by Tsebulya *et al.*<sup>15</sup> on a  $\text{CaB}_6$  single crystal in a limited spectral range and revealing the onset of a plasma edge around  $3500\text{ cm}^{-1}$ . At present, we do not know the origin of this discrepancy.

While Fig. 8(b) gives an overall view of  $\sigma_1(\omega)$ , Fig. 9 emphasizes the mid and far infrared spectral ranges. The central features of Fig. 9 are the absorptions at  $700$  and  $1200\text{ cm}^{-1}$ , observed for 0.5% La-doped  $\text{CaB}_6$  and already identified before in the  $R(\omega)$  spectra. Here it is more obvious that these two absorptions are absent for  $\text{Ca}_{1+\delta}\text{B}_6$  and very much damped for the material with a La concentration of 0.01.

Figure 8(b) also emphasizes the spectral range ( $\omega > 10^4\text{ cm}^{-1}$ ) of the electronic interband transitions, involving mainly  $s$ -,  $p$ - and  $d$ -type bonding-antibonding bands.<sup>2,4</sup> The overall trend and the main features are similar in all compounds. Quite remarkable and rather unexpected is, however, the difference in spectral weight for the three ma-

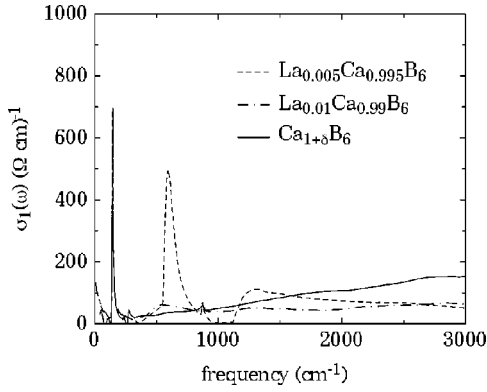


FIG. 9. Expanded view of the mid and far infrared spectral range for the optical conductivity of  $\text{Ca}_{0.99}\text{La}_{0.01}\text{B}_6$ ,  $\text{Ca}_{0.995}\text{La}_{0.005}\text{B}_6$ , and  $\text{Ca}_{1+\delta}\text{B}_6$ .

materials above  $1 \times 10^4 \text{ cm}^{-1}$ . The small differences in chemical composition cannot justify *a priori* such a remarkable change of the electronic interband transitions at energy scales above 10 000 K. Naturally, experimental artifacts, due to surface corrugation, surface oxidation, or surface segregation, might be expected. The surface scattering due to corrugation can be very important at wavelengths of a few micrometers, while surface oxidation and segregation might alter the electronic structure at the surface layers. Nevertheless, we tend to exclude those effects as the reason for our observation, because different samples with the same nominal chemical composition from the same as well as other batches gave equivalent results.

#### IV. DISCUSSION

##### A. Resistivity and specific heat

In comparison with other measured resistivity curves of metal-deficient  $\text{CaB}_6$ ,<sup>1,12</sup> our close to stoichiometric  $\text{Ca}_{1+\delta}\text{B}_6$  sample shows a much stronger  $T$  dependence of the resistivity and, as will be argued later, reveals a semiconductor-type behavior in an extended temperature range. Semiconducting behavior of  $\text{CaB}_6$  has previously been reported by Johnson and Daane.<sup>16</sup> Their measurement were made on polycrystalline material and the resistivity showed an exponential behavior as

$$\rho = \rho_0 \exp(\epsilon/2k_B T) \quad (1)$$

only in the temperature range above 800 K, implying an activation energy  $\epsilon = 0.4 \text{ eV}$ . The authors argued that the deviation from the exponential behavior at lower temperatures resulted from the fact that electron conduction due to impurity atoms was not negligible in comparison with conduction due to thermally excited electrons. The room temperature resistivity of  $\text{CaB}_6$  reported by Johnson and Daane<sup>16</sup> is about two orders of magnitude higher than what we observe for our single-crystalline specimens.

Most important for the understanding of the electronic properties of the alkaline-earth hexaborides is their peculiar electronic energy band structure in the vicinity of the Fermi energy. The calculations of Massida *et al.*<sup>4</sup> suggest a semi-metallic character, due to the overlap of an almost filled valence band with an almost empty conduction band around the

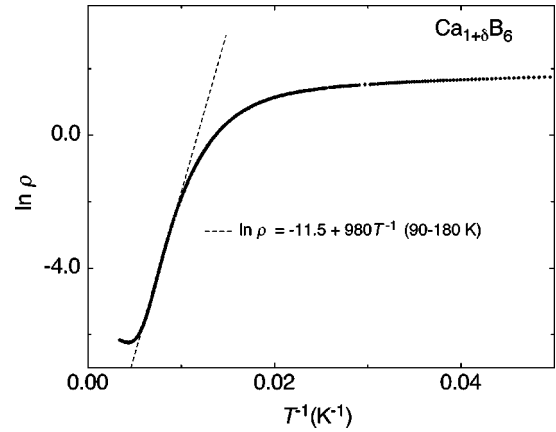


FIG. 10.  $\ln \rho$  vs  $T^{-1}$  of  $\text{CaB}_6$  for temperatures between 5 and 300 K. The dashed line represents the exponential increase in resistivity between 90 and 180 K.

$X$  point in the Brillouin zone. A local maximum in the valence band around the  $\Gamma$  point is responsible for a small peak in the calculated total density of states at about  $-0.3 \text{ eV}$ . Massida *et al.*<sup>4</sup> argued that, due to the low concentration of carriers in the ground state, the high-temperature transport will be dominated by thermally excited quasiparticles and they tentatively identified the energy difference between the highest occupied state around the  $\Gamma$  point and the Fermi level with the activation energy of  $0.4 \text{ eV}$  quoted by Johnson and Daane.<sup>16</sup> However, it should be noticed that the details of the band structure depend rather sensitively on the choice of the potential in the Kohn-Sham<sup>17</sup> equation. Local density approximation (LDA) calculations<sup>4,6</sup> yield a small band overlap of about  $E_G = -200 \text{ meV}$  at the Fermi energy around the  $X$  point in the Brillouin zone, whereas the modified LDA+ $U$  method yields a small band gap of about  $E_G = 150 \text{ meV}$ .

Our measurements on  $\text{Ca}_{1+\delta}\text{B}_6$  reveal a strong  $T$  dependence of the resistivity below 230 K, which is well illustrated when plotting  $\ln \rho$  vs  $T^{-1}$  as in Fig. 10. If we assume that the change in resistivity is due to a thermally activated process, then a linear fit in the appropriate temperature regime provides, according to Eq. (1), an estimate of the activation energy  $\epsilon$ . The dashed line in Fig. 10 represents such a fit in the temperature range between 170 and 70 K, leading to an activation energy  $\epsilon = 168 \text{ meV}$ , or its equivalent in temperature  $T = 1960 \text{ K}$ . This activation energy is considerably smaller than the calculated energy difference between the local maximum in the valence band around the  $\Gamma$  point and the Fermi energy.<sup>4</sup> Therefore we tentatively associate the measured activation energy with a band gap at the  $X$  point of the Brillouin zone.

The energy gap value of  $\epsilon = 168 \text{ meV}$  for the  $\text{Ca}_{1+\delta}\text{B}_6$  material is rather close to the theoretical prediction of Zhitomirsky *et al.*<sup>6</sup> who, with a modified LDA+ $U$  calculation, found a simple band gap with a value of  $150 \text{ meV}$ . However, a simple band gap seems not to be compatible with the observed properties at low temperatures discussed below. We therefore assume that our result has to be discussed in an excitonic scenario,<sup>6</sup> where an originally overlapping band structure<sup>4</sup> at the  $X$  point of the Brillouin zone develops into an excitonic gap. Assuming this scenario to be valid, we attribute the measured gap of  $168 \text{ meV}$  to the excitonic gap (see also Sec. IV B).

Both the low-temperature resistivity and the specific heat data indicate a crossover phenomenon occurring below 0.5 K. The main characteristics are a strong decrease of the resistivity below 0.4 K, a  $T^3$  dependence of the resistivity below 150 mK, the suppression of the resistivity decrease by moderate magnetic fields, and a maximum in the specific heat at 0.3 K, with a subsequent decrease, linear in temperature, below 0.15 K. Similar features have previously been reported for  $\text{SrB}_6$ .<sup>2</sup> Even though there is no understanding yet of the low-temperature behavior of the resistivity and the specific heat in an excitonic scenario, it has been conjectured<sup>6</sup> that low-lying magnetic collective excitations in the stoichiometric compound, which are the spin waves of the triplet exciton condensate, might be observed. We therefore tentatively associate the low-temperature behavior in the resistivity and the specific heat with these low-lying magnetic excitations.

We now turn our attention to the magnetoresistance  $[\rho(H) - \rho(0)]/\rho(0)$  of the  $\text{Ca}_{1+\delta}\text{B}_6$  sample at temperatures below 1.2 K. Understanding the influence of applied magnetic fields on the resistivity at low temperatures is not straightforward. In the case of simple metals a positive transverse magnetoresistance is usually observed. For low applied magnetic fields a quadratic magnetic field dependence is expected, whereas for high magnetic fields a saturation or a quadratic behavior may be observed, depending on the electronic orbits being closed or open.<sup>18</sup> In our  $\text{Ca}_{1+\delta}\text{B}_6$  sample two different regimes can be distinguished. First, the magnetoresistance increases very fast and already reaches a maximum at about 13 kOe. At 100 mK this maximum can be as high as 65%. For higher applied magnetic fields the magnetoresistance decreases slowly, without reaching negative values in the covered magnetic field and temperature range. This seems to imply two different contributions to the transverse magnetoresistance. In fact, we observe that up to 13 kOe the application of magnetic fields suppresses the reduction of the resistivity (see Fig. 2) and the temperature dependence weakens, i.e.,  $\beta$  tends to zero (see inset of Fig. 2). Above 13 kOe, however, the entire resistivity curve below 0.4 K shifts to lower values, implying a negative contribution to the transverse magnetoresistance in our  $\text{CaB}_6$  sample. Anomalous magnetoresistances have been observed previously in weakly disordered electronic systems in connection with weak localization,<sup>19</sup> but it seems very unlikely that this theory will apply in our highly ordered but weakly conducting system. If we assume that the low-temperature properties of  $\text{Ca}_{1+\delta}\text{B}_6$  are dominated by low-lying magnetic excitations as mentioned above, the observed magnetoresistance might then be due to the influence of the applied magnetic field on these excitations. To our knowledge, however, the influence of external magnetic fields on the resistivity of a Bose condensate of excitons has not yet been considered theoretically.

A comparison of the resistivities of  $\text{Ca}_{1+\delta}\text{B}_6$  and La-doped  $\text{CaB}_6$  reveals that at high temperatures, above 230 K, they exhibit a similar temperature dependence (inset of Fig. 4) and that only below 230 K is the behavior distinctly different. The low-temperature behavior of the resistivity for  $\text{Ca}_{1+\delta}\text{B}_6$ , with a maximum around 0.4 K and a reduction towards lower temperatures, is very different from the much smaller resistivity for La-doped  $\text{CaB}_6$ , with a minimum around 25 K and a small increase towards lower tempera-

tures. In the specific heat measurements, however, no appreciable differences were noted (see Fig. 5). This observation may indicate that the low-energy excitations of these systems are not significantly affected by doping.

## B. Optical data

Unlike the dc conductivity data, the optical spectra do not reveal any dramatic change between  $\text{Ca}_{1+\delta}\text{B}_6$  and the La-doped material. The enhanced metallic behavior of the La-doped compounds is, as expected, confirmed by a slightly higher reflectivity in the far infrared, which allows a so-called Hagen-Rubens extrapolation using  $\sigma_{\text{dc}}$  values in agreement with the transport result (Fig. 4). Even in the La-doped samples the FIR phonon modes and the absorptions at 700 and 1200  $\text{cm}^{-1}$  are strong enough to screen the plasma resonance so that a plasma edge is recognized in the reflectivity at frequencies lower than the phonon mode excitation at 150  $\text{cm}^{-1}$ . In the infrared the central features of the optical reflectivity of the 0.5% La-doped material (Fig. 8) are the absorptions at 700 and 1200  $\text{cm}^{-1}$  (87 meV and 150 meV). These two absorptions are substantially damped in the 1% material. It has been conjectured<sup>20</sup> that these absorptions could be, within the excitonic scenario, the optical evidence for the band gaps of minority and majority spin charge carriers. It seems most surprising that at the same energies no evidence for absorption is observed in the  $\text{Ca}_{1+\delta}\text{B}_6$  data. Instead, in the latter we observe two narrow absorptions at 240 and 275  $\text{cm}^{-1}$ , respectively [see inset of Fig. 8(a)]. Even more puzzling is the fact that minor changes in the chemical composition provoke substantial variations in  $R(\omega)$ . The origin of the two absorptions in the  $\text{Ca}_{1+\delta}\text{B}_6$  compound remains unclear at present. Our dc transport and optical data, together with the model of Zhitomirsky *et al.*,<sup>6</sup> seem to imply the following scenario for stoichiometric  $\text{CaB}_6$  and its La-doped alloys.

In the case of stoichiometric  $\text{CaB}_6$ , the model calculations<sup>6</sup> suggest a single energy gap, the same for spin-up and spin-down quasiparticles. Evidence for this energy gap is clearly observed in the resistivity data with  $\epsilon = 168$  meV, i.e., within 10% of the value following from the theoretical interpretation<sup>6</sup> of the optical data of the 0.5% La-doped material. In the spectrum of stoichiometric  $\text{CaB}_6$ , the corresponding gap absorption seems to be hidden by a broad background contribution to  $\sigma_1(\omega)$ , which increases almost linearly with  $\omega$  in this frequency region (Fig. 9).

In the case of the La-doped  $\text{CaB}_6$ , the model calculations<sup>6</sup> suggest two energy gaps for small La doping, corresponding to the energy gap for spin-up and spin-down quasiparticles, respectively (see Fig. 2 in Ref. 6). The calculations seem to overestimate the effect of doping. Figure 2 of Ref. 6 implies that already at 0.7% La doping ferromagnetism should be quenched, in contradiction with experiment.<sup>1</sup> In spite of this deficiency of the model we use its implications for the following brief discussion. In the optical conductivity two distinct absorptions are observed. The one at about 1200  $\text{cm}^{-1}$  (corresponding to 150 meV) may tentatively be associated with the energy gap for spin-up quasiparticles. This energy gap is very similar in size to the gap obtained from the resistivity measurements of the  $\text{Ca}_{1+\delta}\text{B}_6$  sample, discussed above. This is in agreement with the model of Ref. 6, sug-

gesting an almost doping-independent energy gap for spin-up quasiparticles. The absorption at about  $700\text{ cm}^{-1}$ , however, may tentatively be associated with the energy gap for spin-down quasiparticles. Comparing the optical conductivities of the 0.5% and 1% La-doped samples, we note that for the higher La concentration the absorption is not only broadened but also shifted toward lower frequencies, in agreement with the model calculations<sup>6</sup> showing a reduction of the energy gap for spin-down quasiparticles as a function of the doping. The resistivity measurements of the La-doped  $\text{CaB}_6$  samples seem to be dominated by extra conduction electrons, also observed in the optical data as a small Drude weight at zero frequency, such that the activation of additional charge carriers is irrelevant and therefore not observed in the resistivity measurements.

## V. SUMMARY

We have presented a study of transport, thermal, and optical properties of  $\text{CaB}_6$  and La-doped  $\text{CaB}_6$ , which illustrates the strong sensitivity of alkaline-earth hexaborides to

metal vacancies and doping. Close to stoichiometric  $\text{CaB}_6$  exhibits quasisemiconducting behavior in an extended temperature range below 230 K. We tentatively associate this behavior with the opening of an excitonic gap at the Fermi energy of  $\text{CaB}_6$ , as suggested by model calculations of Zhitomirsky *et al.*<sup>6</sup> Support for this approach is gained from measurements of the optical properties. In La-doped  $\text{CaB}_6$  two absorption peaks around 700 and  $1200\text{ cm}^{-1}$  are observed, which may be the optical evidence for the band gaps of minority and majority spin charge carriers. Furthermore, we tentatively associate the low-temperature behavior in the resistivity and the specific heat with low-lying magnetic excitations in the Bose condensate of excitons.

## ACKNOWLEDGMENTS

We are grateful to M. E. Zhitomirsky, T. M. Rice, and R. Monnier for stimulating discussions. This work was financially supported in part by the Schweizerische Nationalfonds zur Förderung der Wissenschaftlichen Forschung.

<sup>1</sup>D.P. Young, D. Hall, M.E. Torelli, J.L.S.Z. Fisk, J.D. Thompson, H.R. Ott, S.B. Oseroff, R.G. Goodrich, and R. Zysler, *Nature (London)* **397**, 412 (1999).

<sup>2</sup>H.R. Ott, M. Chernikov, E. Felder, L. Degiorgi, E.G. Moshopoulou, J.L. Sarrao, and Z. Fisk, *Z. Phys. B: Condens. Matter* **102**, 337 (1997).

<sup>3</sup>H.R. Ott, J.L. Gavilano, B. Ambrosini, P. Vonlanthen, E. Felder, L. Degiorgi, D.P. Young, Z. Fisk, and R. Zysler, *Physica B* **281&282**, 423 (2000).

<sup>4</sup>S. Massidda, A. Continenza, T.M. de Pascale, and R. Monnier, *Z. Phys. B: Condens. Matter* **102**, 83 (1997).

<sup>5</sup>D. Ceperley, *Nature (London)* **397**, 386 (1999).

<sup>6</sup>M.E. Zhitomirsky, T.M. Rice, and V.I. Anisimov, *Nature (London)* **402**, 251 (1999).

<sup>7</sup>V. Barzykin and L.P. Gor'kov, *Phys. Rev. Lett.* **84**, 2207 (2000).

<sup>8</sup>L. Balents and C.M. Varma, *Phys. Rev. Lett.* **84**, 1264 (2000).

<sup>9</sup>M.E. Zhitomirsky and T.M. Rice, cond-mat/9910272 (unpublished).

<sup>10</sup>K.E. Spear, in *Boron and Refractory Borides*, edited by V.I. Matkovich (Springer, Berlin, 1977), p. 439.

<sup>11</sup>F. Wooten, *Optical Properties of Solids* (Academic Press, New York, 1972).

<sup>12</sup>S. Paschen, D. Pushin, M. Schlatter, P. Vonlanthen, H.R. Ott, D.P. Young, and Z. Fisk, *Phys. Rev. B* **61**, 4174 (2000).

<sup>13</sup>W. Bührer and W. Hälgl, *Phys. Status Solidi B* **46**, 679 (1971).

<sup>14</sup>L. Degiorgi, E. Felder, H.R. Ott, J.L. Sarrao, and Z. Fisk, *Phys. Rev. Lett.* **79**, 5134 (1997).

<sup>15</sup>G. Tsebulya, G.K. Kozina, A.P. Zakharchuk, A.V. Kovalev, and E.M. Dudnik, *Powder Metall. Met. Ceram.* **36**, 413 (1997).

<sup>16</sup>R.W. Johnson and A.H. Daane, *J. Chem. Phys.* **38**, 425 (1963).

<sup>17</sup>W. Kohn and L.J. Sham, *Phys. Rev.* **140**, A1133 (1965).

<sup>18</sup>G.T. Meaden, *Electrical Resistance of Metals* (Heywood Books, London, 1965).

<sup>19</sup>P.A. Lee and T.V. Ramakrishnan, *Rev. Mod. Phys.* **57**, 287 (1985).

<sup>20</sup>T. M. Rice (private communication).